Electronic Supplementary Information for

Excitonic cuprophilic interactions in one-dimensional hybrid organic-inorganic crystal

Nahid Hassan,[a] Suneetha Nagaraja,[b] Sauvik Saha,[a] Kartick Tarafder[b] & Nirmalya Ballav*[a]

[a]Department of Chemistry, Indian Institute of Science Education and Research, Dr. Homi Bhabha Road, Pune – 411 008, India

[b]Department of Physics, National Institute of Technology Karnataka, Surathkal, Mangalore – 575 025, India.
*Corresponding author. Email: nballav@iiserpune.ac.in

Table S1. Crystal data and structure refinement for the $(TMA)Cu_2Br_3$ system.

Empirical Formula	$C_4H_{12}Br_3Cu_2N$
Formula Weight	440.96
Temperature/K	296(2)
Crystal System	orthorhombic
Space group	Pnma
a/Å	16.359(3)
b/Å	6.5479(11)
c/Å	9.5918(17)
α/°	90
β/°	90
γ/°	90
Volume/Å^3	1027.5(3)
Z	4
Density (ρ_{calc})/g.cm^{-3}	2.851
Absorption coefficient (μ)/mm^{-1}	15.741
F(000)	824.0
Radiation	MoKα (λ = 0.71073 Å)
Θ range for data collection/°	2.46 to 28.34
Index ranges	$-21 \leq h \leq 21$, $-8 \leq k \leq 8$, $-12 \leq l \leq 12$
Reflections collected	19735
Independent reflections	1392 [$R_{int} = 0.0692$, $R_{sigma} = 0.0275$]
Coverage of independent reflections	99.9%
Function minimized	$\Sigma\, w(F_o^2 - F_c^2)^2$
Data/restraints/parameters	1392/0/59
Goodness-of-fit on F^2	0.860
Final R indexes [I > 2σ(I)]	1325 data, $R_1 = 0.0241$, $wR_2 = 0.0944$
Final R indexes [all data]	$R_1 = 0.0258$, $wR_2 = 0.0971$
Largest diff. peak and hole/ eÅ^{-3}	0.897 and -0.873
R.M.S. deviation from mean/ eÅ^{-3}	0.182

Table S2. Fractional Atomic Coordinates for the (TMA)Cu_2Br_3 single crystal.

Atom	***x***	***y***	***z***
Br1	0.45759(2)	0.75	0.63059(3)
Cu1	0.42516(2)	0.49878(5)	0.43192(4)
Br2	0.39680(3)	0.75	0.24955(4)
Br3	0.32552(2)	0.25	0.50566(4)
N1	0.6468(2)	0.75	1.0272(3)
C2	0.6545(2)	0.9352(5)	1.1172(3)
C3	0.5657(2)	0.75	0.9569(4)
C4	0.7123(3)	0.75	0.9189(4)

Table S3. Bond lengths and bond angles in the (TMA)Cu_2Br_3 single crystal.

Atom	Atom	Length/Å	Atom	Atom	Atom	Angle/°
Cu1	Br2	2.4456	Cu1	Br1	Cu1	65.08
Cu1	Br3	2.4106	Cu1	Br1	Cu1	112.57
Cu1	Cu1	2.7752(6)	Cu1	Br1	Cu1	79.49
Cu1	Br1	2.5869	Cu1	Br1	Cu1	78.06
Cu1	Br1	2.5727	Br1	Cu1	Br2	97.98
N1	C2	1.494	Br1	Cu1	Br3	110.74
N1	C3	1.488	Br1	Cu1	Cu1	57.71
N1	C4	1.492	Br1	Cu1	Br1	114.92
---	---	---	Br2	Cu1	Br3	122.42
---	---	---	Br2	Cu1	Cu1	120.01
---	---	---	Br2	Cu1	Br1	113.48
---	---	---	Br3	Cu1	Cu1	117.54
---	---	---	Br3	Cu1	Br1	98.27
---	---	---	Cu1	Cu1	Br1	57.21
---	---	---	Cu1	Br2	Cu1	84.54
---	---	---	Cu1	Br3	Cu1	85.03
---	---	---	C2	N1	C3	109.7
---	---	---	C2	N1	C4	110
---	---	---	C2	N1	C2	108.5
---	---	---	C3	N1	C4	108.9

Table S4. Symmetry operators for the (TMA)Cu_2Br_3 single crystal.

Symm. Op.	Description	Detailed Description	Order
x,y,z	Identity	Identity	1
1/2-x,y,1/2+z	Screw axis (2-fold)	2-fold screw axis with direction [0, 0, 1] at 1/4, 0, z with screw component [0, 0, 1/2]	2
-x,1/2+y,-z	Screw axis (2-fold)	2-fold screw axis with direction [0, 1, 0] at 0, y, 0 with screw component [0, 1/2, 0]	2
1/2+x,1/2-y,1/2-z	Screw axis (2-fold)	2-fold screw axis with direction [1, 0, 0] at x, 1/4, 1/4 with screw component [1/2, 0, 0]	2
-x,-y,-z	Inversion centre	Inversion at [0, 0, 0]	2
1/2+x,y,1/2-z	Glide plane	Glide plane perpendicular to [0, 0, 1] with glide component [1/2, 0, 0]	2
x,1/2-y,z	Mirror plane	Mirror plane perpendicular to [0, 1, 0]	2
1/2-x,1/2+y,1/2+z	Glide plane	Glide plane perpendicular to [1, 0, 0] with glide component [0, 1/2, 1/2]	2

Table S5. Crystal data and structure refinement for the $(TMA)Ag_2Br_3$ system.

Empirical Formula	$C_4H_{12}Br_3Ag_2N$
Formula Weight	529.62
Temperature/K	150(2)
Crystal System	orthorhombic
Space group	Pnma
a/Å	16.535(2)
b/Å	7.0771(9)
c/Å	9.6517(11)
α/°	90
β/°	90
γ/°	90
Volume/Å^3	1129.4(2)
Z	4
Density (ρ_{calc})/g.cm^{-3}	3.115
Absorption coefficient (μ)/mm^{-1}	14.022
F(000)	968.0
Radiation	MoKα (λ = 0.71073 Å)
Θ range for data collection/°	2.46 to 25.03
Index ranges	$-19 \leq h \leq 19$, $-8 \leq k \leq 8$, $-10 \leq l \leq 11$
Reflections collected	15396
Independent reflections	1087 [$R_{int} = 0.0448$, $R_{sigma} = 0.0179$]
Coverage of independent reflections	99.8%
Function minimized	$\Sigma\, w(F_o^2 - F_c^2)^2$
Data/restraints/parameters	1087/0/58
Goodness-of-fit on F^2	1.219
Final R indexes [$I > 2\sigma(I)$]	1009 data, $R_1 = 0.0222$, $wR_2 = 0.0480$

Final R indexes [all data]	$R_1 = 0.0252$, $wR_2 = 0.0489$
Largest diff. peak and hole/ eÅ^{-3}	0.598 and -1.401
R.M.S. deviation from mean/ eÅ^{-3}	0.265

Table S6. Fractional Atomic Coordinates for the (TMA)Ag_2Br_3 single crystal.

Atom	***x***	***y***	***z***
Ag1	0.42040(2)	0.49756(3)	0.57957(3)
Br1	0.45040(3)	0.75	0.36287(4)
Br2	0.39770(3)	0.75	0.77831(5)
Br3	0.31064(3)	0.25	0.50893(6)
N1	0.3549(2)	0.25	0.0374(4)
C11	0.3552(3)	0.4219(4)	0.1275(4)
C12	0.2820(3)	0.25	-0.0531(6)
C13	0.4285(3)	0.25	-0.0506(5)

Table S7. Bond lengths and bond angles in the (TMA)Ag_2Br_3 single crystal.

Atom	Atom	Length/Å	Atom	Atom	Atom	Angle/°
Ag1	Br1	2.795	Br1	Ag1	Br2	97.81
Ag1	Br2	2.648	Br1	Ag1	Br3	110.89
Ag1	Br3	2.6131	Br1	Ag1	Ag1	57.48
N1	C11	1.495	Br1	Ag1	Br1	114.23
N1	C12	1.489	Br2	Ag1	Br3	122.88
N1	C13	1.484	Br2	Ag1	Ag1	118.67
C11	H11A	0.98	Br2	Ag1	Br1	112.59
C11	H11B	0.98	Br3	Ag1	Ag1	118.42
C11	H11C	0.98	Br3	Ag1	Br1	99.27
C12	H12A	0.981	Ag1	Ag1	Br1	56.75
C12	H12B	0.98	Ag1	Br1	Ag1	65.77
C12	H12C	0.98	Ag1	Br1	Ag1	112.61
C13	H13A	0.98	Ag1	Br1	Ag1	79.46
C13	H13B	0.98	Ag1	Br1	Ag1	76.88
C13	H13C	0.98	Ag1	Br2	Ag1	84.86
---	---	---	Ag1	Br3	Ag1	84.21
---	---	---	C11	N1	C12	110.1
---	---	---	C11	N1	C13	109.3
---	---	---	C11	N1	C11	108.9
---	---	---	C12	N1	C13	109.2

Table S8. Symmetry operators for the (TMA)Ag_2Br_3 single crystal.

Symm. Op.	Description	Detailed Description	Order
x,y,z	Identity	Identity	1
1/2-x,-y,1/2+z	Screw axis (2-fold)	2-fold screw axis with direction [0, 0, 1] at 1/4, 0, z with screw component [0, 0, 1/2]	2
-x,1/2+y,-z	Screw axis (2-fold)	2-fold screw axis with direction [0, 1, 0] at 0, y, 0 with screw component [0, 1/2, 0]	2
1/2+x,1/2-y,1/2-z	Screw axis (2-fold)	2-fold screw axis with direction [1, 0, 0] at x, 1/4, 1/4 with screw component [1/2, 0, 0]	2
-x,-y,-z	Inversion centre	Inversion at [0, 0, 0]	2
1/2+x,y,1/2-z	Glide plane	Glide plane perpendicular to [0, 0, 1] with glide component [1/2, 0, 0]	2
x,1/2-y,z	Mirror plane	Mirror plane perpendicular to [0, 1, 0]	2
1/2-x,1/2+y,1/2+z	Glide plane	Glide plane perpendicular to [1, 0, 0] with glide component [0, 1/2, 1/2]	2

Table S9. Light intensity vs Responsivity of (TMA)Cu_2Br_3 device at 1 V bias under 450 nm light

Light Intensity (mW.mm^{-2})	**Responsivity, R (nA/W)**
10	0.469
20	0.323
30	0.268
40	0.240
50	0.235

Photoresponsivity (R) is calculated by the following expression:

$$R = \frac{I_{photo}}{(P * A)}$$

where I_{photo} refers to $(I_{light} - I_{dark})$, P is the incident light intensity, A stands for the active area between the contact electrodes (A = 1.90 mm x 0.37 mm x π).

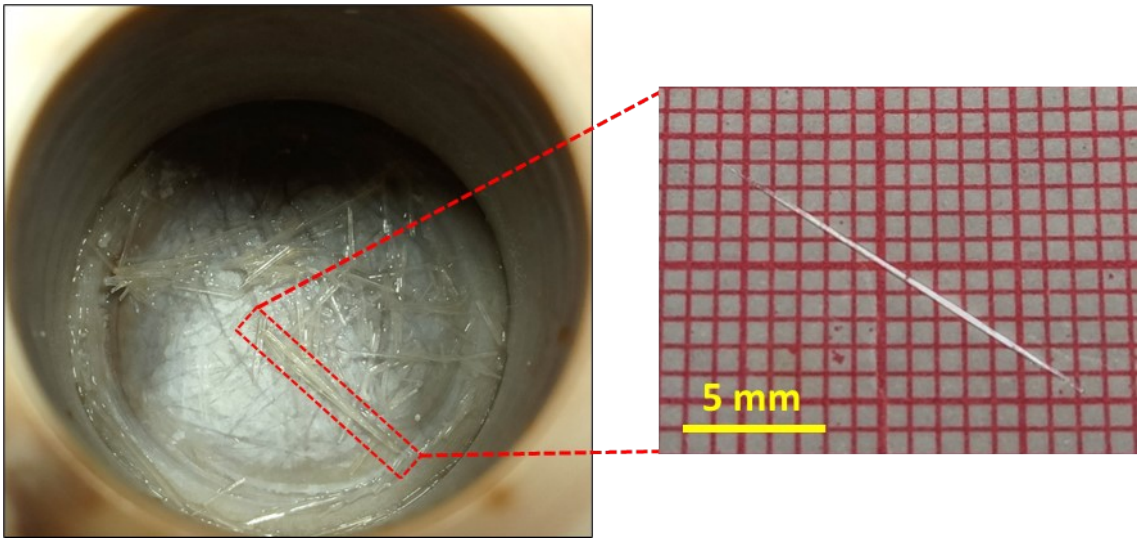

Figure S1. Optical image of (TMA)Cu_2Br_3 single crystals grown in a Teflon lined autoclave (left panel) and zoomed-in view of a needle-like single crystal with dimensions of approximately 16 mm x 0.5 mm (right panel).

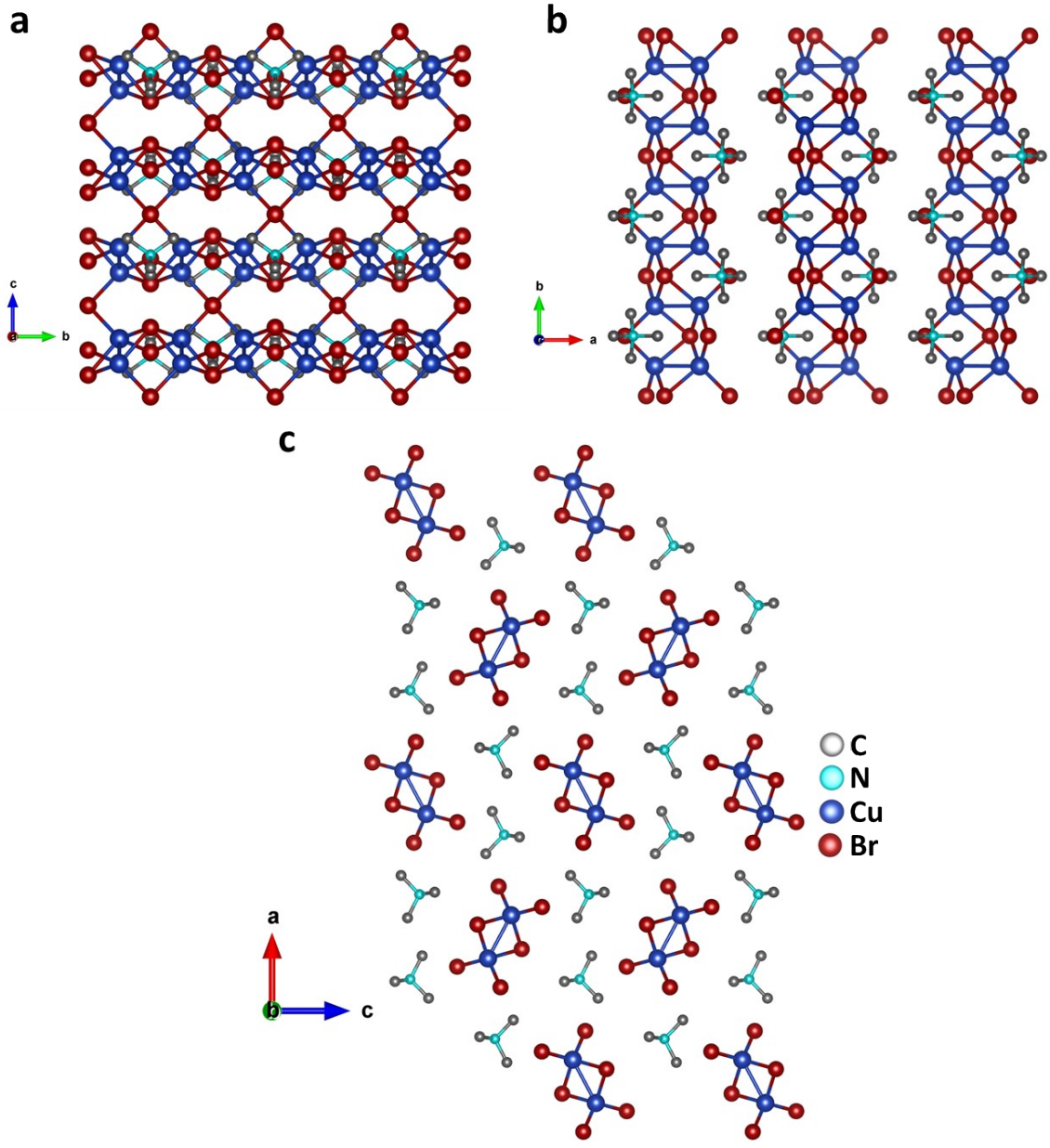

Figure S2. Crystal structure of $(TMA)Cu_2Br_3$ viewed along (a) a-axis, (b) c-axis, and (c) b-axis. H atoms are omitted for clarity. Each $(Cu_2Br_3)_n^{n-}$ inorganic ladder is surrounded by six stacks of TMA^+ cations.

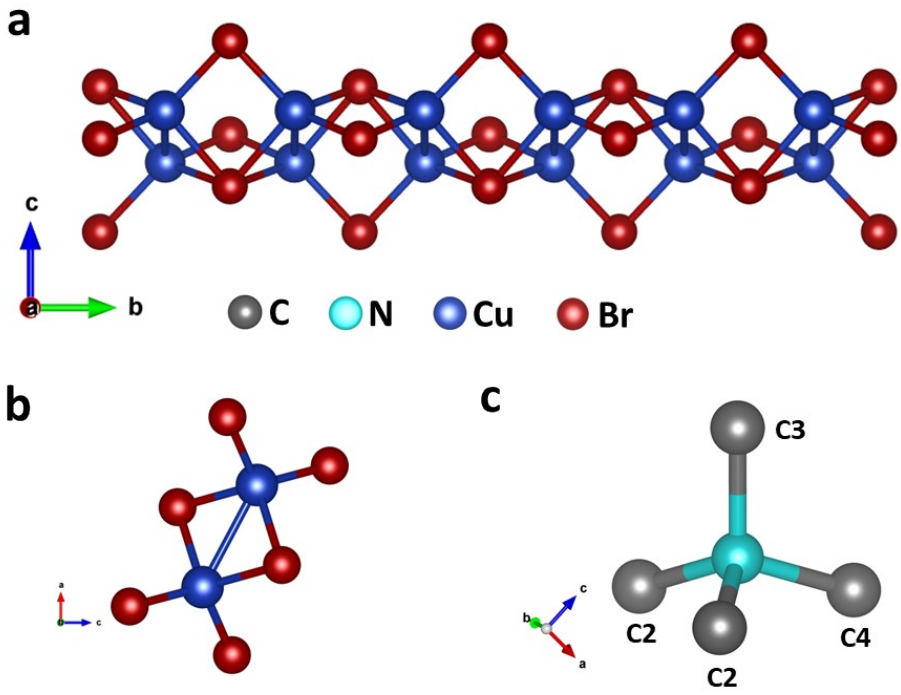

Figure S3. Polymeric chain of $(Cu_2Br_3)_n^{n-}$ anions viewed along (a) a-axis, (b) b-axis. (c) Zoomed-in view of tetramethylammonium (TMA) cation. Carbon, nitrogen, copper, and bromine atoms are represented by grey, cyan, blue, and red coloured spheres.

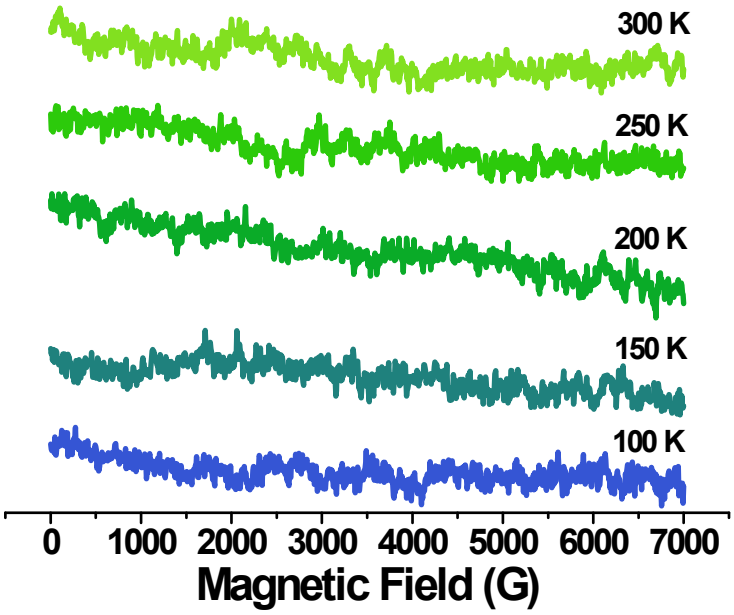

Figure S4. Temperature-dependent EPR spectra at X-band recorded for the (TMA)Cu_2Br_3 system in the temperature range from 100 K to 300 K.

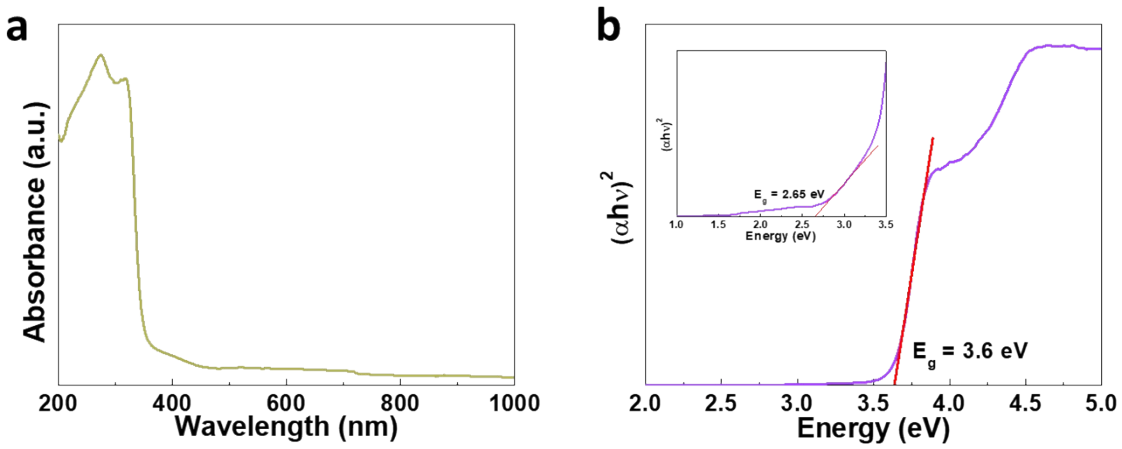

Figure S5. (a) Room temperature solid-state UV-visible absorption (DRS) spectrum of (TMA)Cu_2Br_3. (b) Tauc plot of (TMA)Cu_2Br_3 showing the band gap (inset shows the band gap corresponding to the lower energy region).

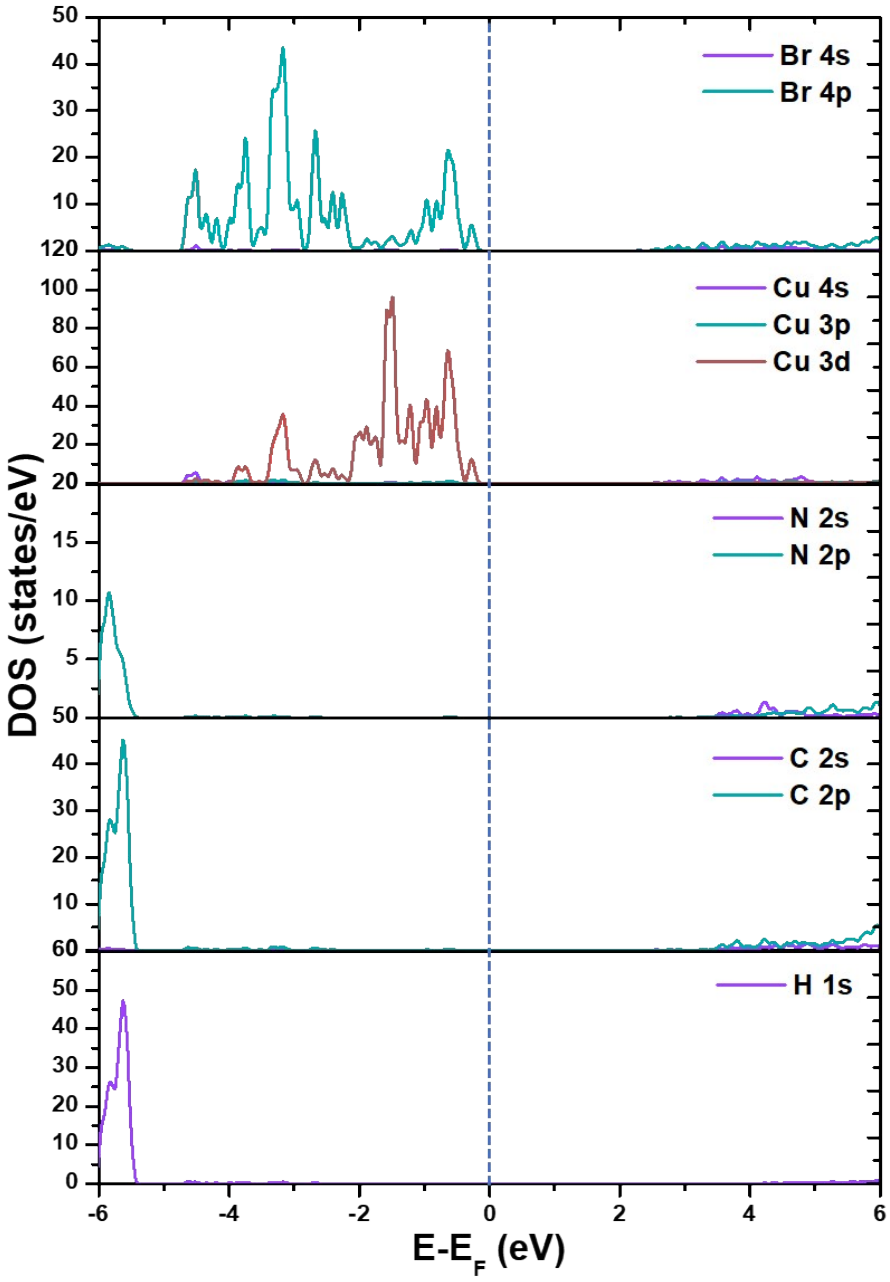

Figure S6. Orbital resolved partial density of state (DOS) plots for H, C, N, Cu and Br atoms. Fermi energy (E_F) marked by dotted blue line.

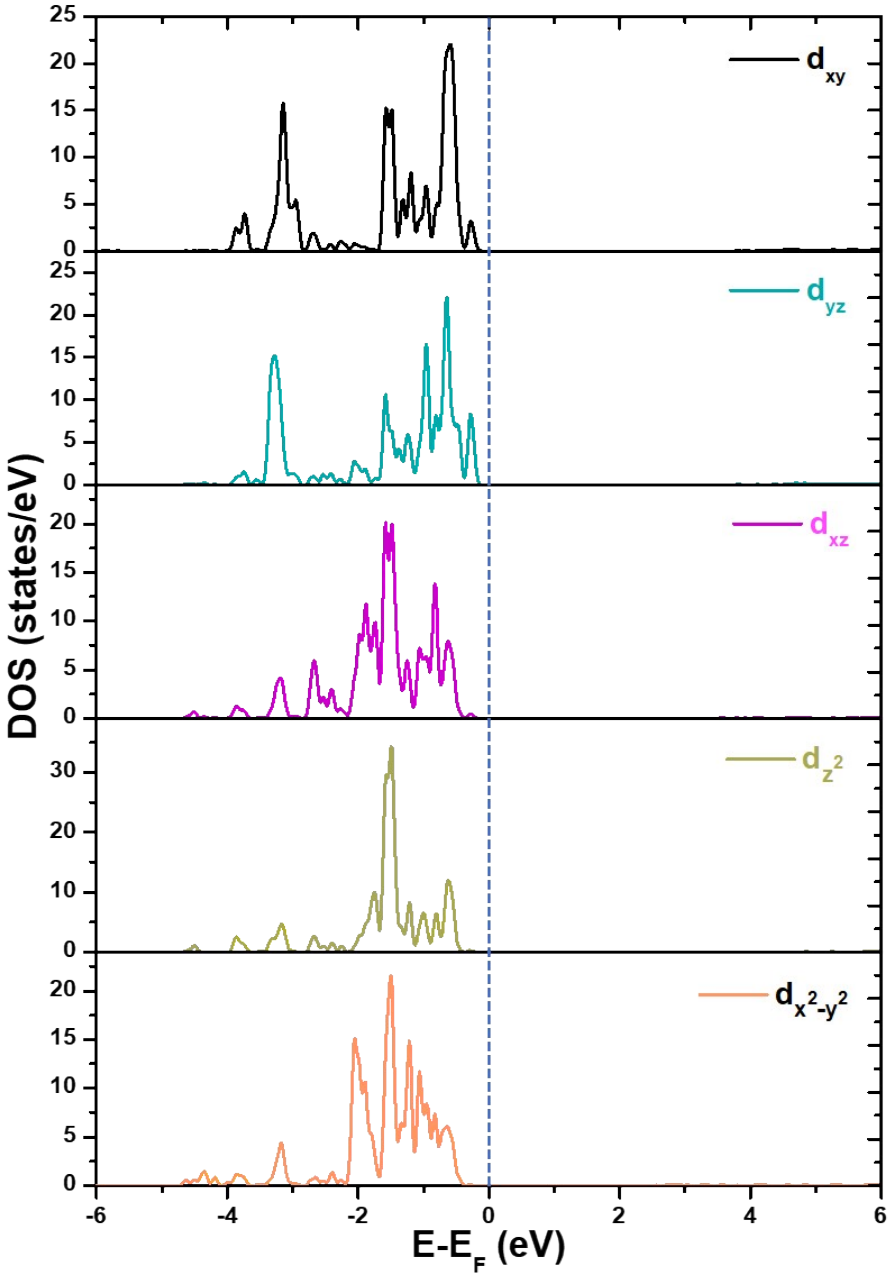

Figure S7. d-orbital resolved partial density of state (DOS) plots for Cu 3d. Fermi energy (E_F) marked by dotted blue line.

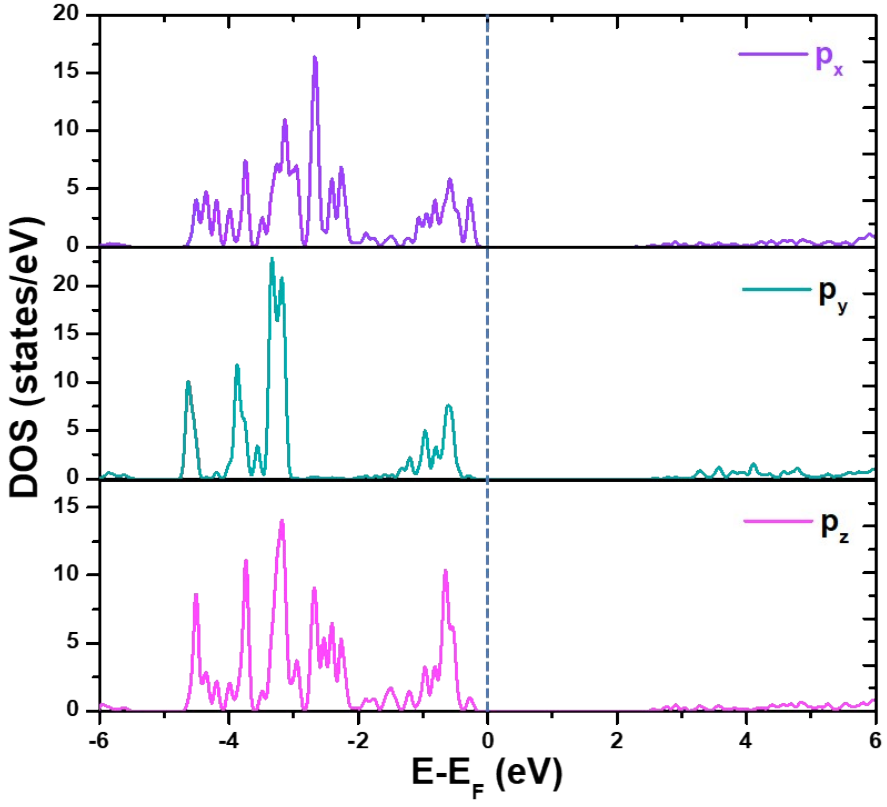

Figure S8. p-orbital resolved partial density of state (DOS) plots for Br 4p. Fermi energy (E_F) marked by dotted blue line.

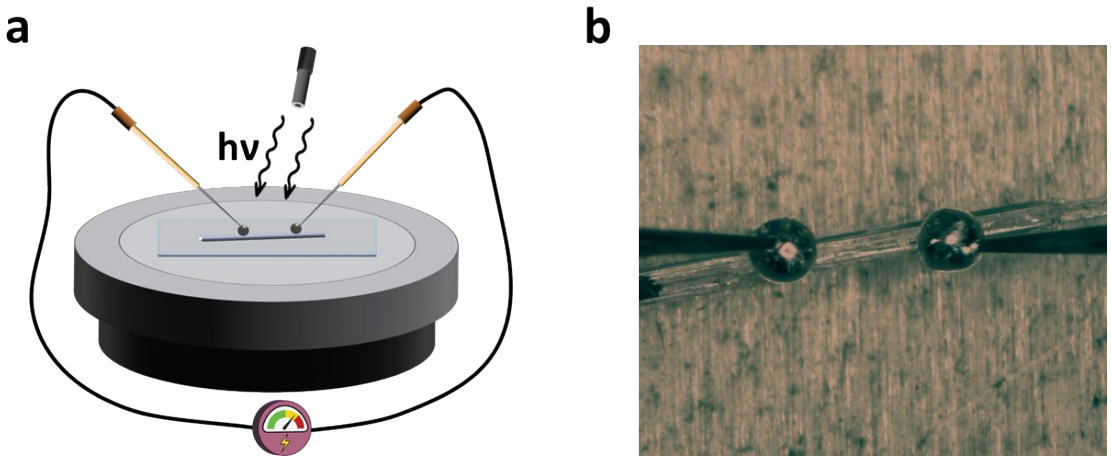

Figure S9. (a) Schematic representation of the measurements of photoresponsivity of the (TMA)Cu_2Br_3 system and (b) optical image of the single crystal device with EGaIn contact electrodes.

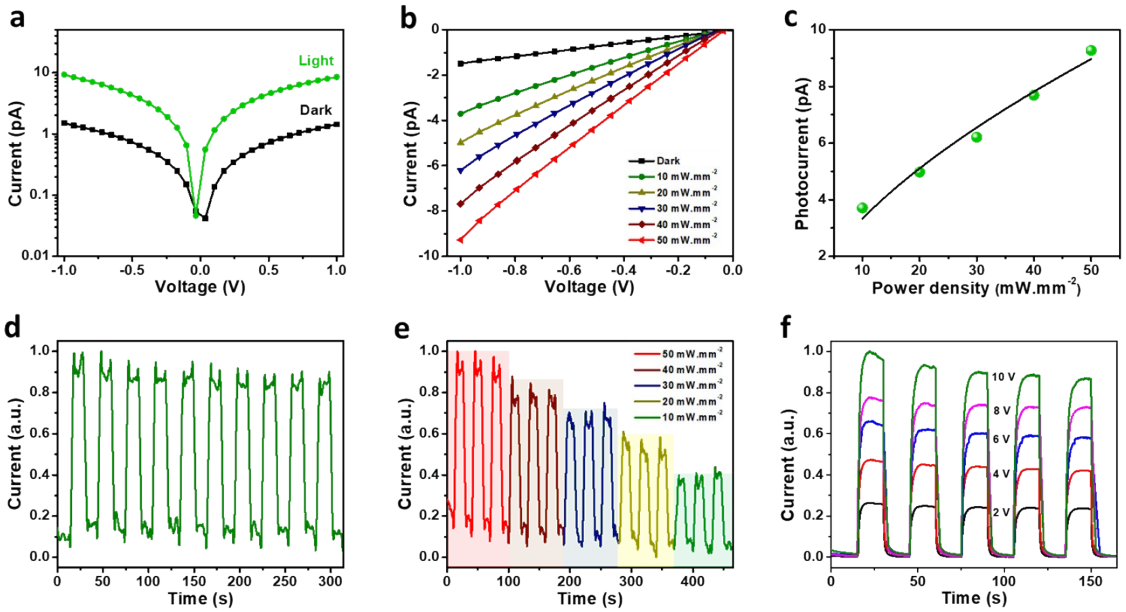

Figure S10. (a) *I-V* curves in dark and under light intensity of 50 mW.mm^{-2} (532 nm). (b) *I-V* curves under varying light intensity ranging from 10 mW.mm^{-2} to 50 mW.mm^{-2}. (c) Plot of photocurrent variation with incident light intensity. Data points are fitted using the power law. (d) Time dependent photocurrent response under 50 mW.mm^{-2} light intensity at 0 V bias (normalized plots). Current as a function of time (*I*-t) curves at different (e) light irradiation intensities (0 V bias) (normalized plots) and (f) bias voltages (50 mW.mm^{-2}) (normalized plots).

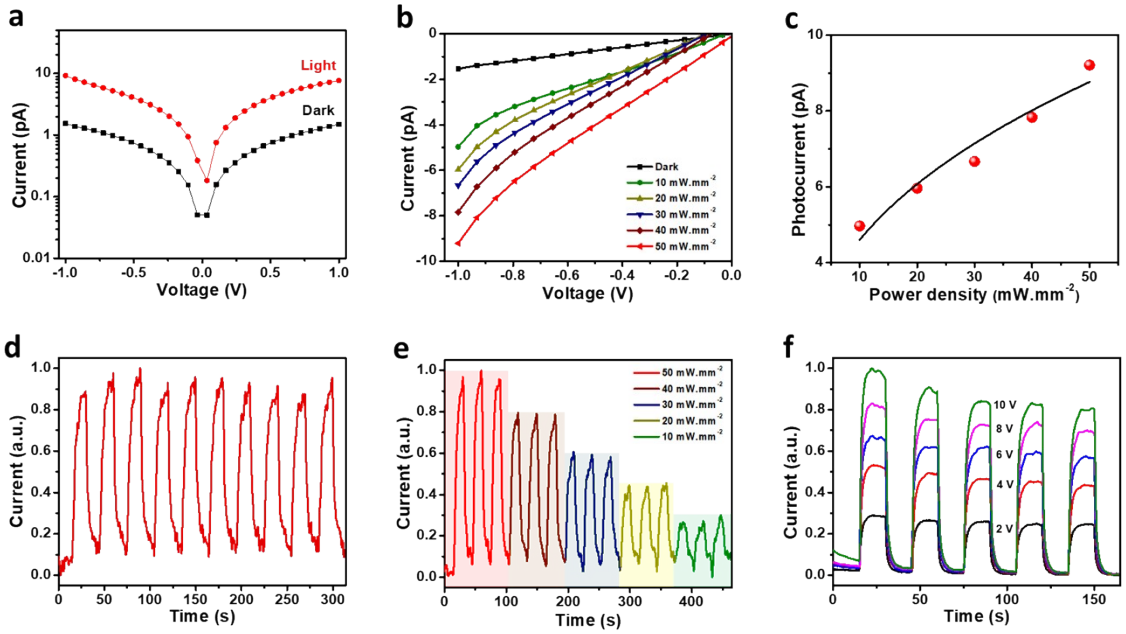

Figure S11. (a) *I-V* curves in dark and under light intensity of 50 mW.mm^{-2} (808 nm). (b) *I-V* curves under varying light intensity ranging from 10 mW.mm^{-2} to 50 mW.mm^{-2}. (c) Plot of photocurrent variation with incident light intensity. Data points are fitted using the power law. (d) Time dependent photocurrent response under 50 mW.mm^{-2} light intensity at 0 V bias (normalized plots). Current as a function of time (*I*-t) curves at different (e) light irradiation intensities (0 V bias) (normalized plots) and (f) bias voltages (50 mW.mm^{-2}) (normalized plots).

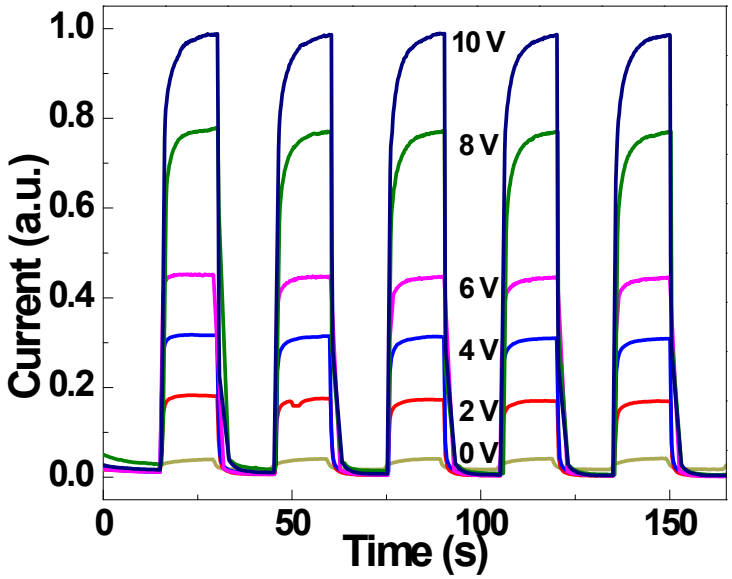

Figure S12. Current as a function of time (*I*-t) curves at different bias voltages (0 V to 10 V) (450 nm, 50 mW.mm^{-2}). The data sets are normalized with respect to the values at 10 V.

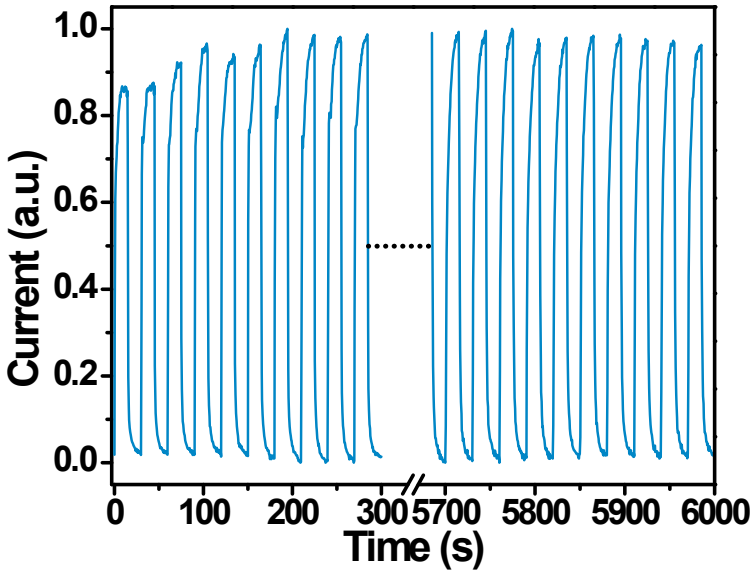

Figure S13. *I*-t plots of the crystal device for 200 continued cycles at 0 V bias under 50 mW.mm^{-2} light intensity (450 nm), showing excellent cycling stability and reversibility.

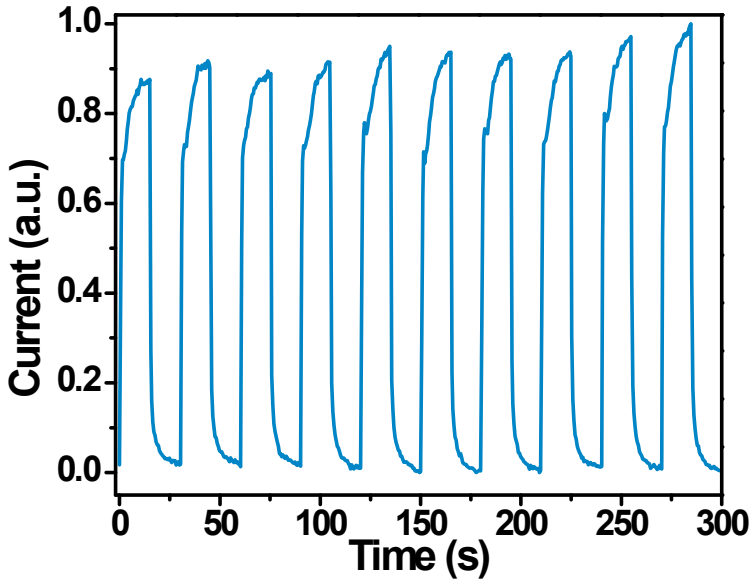

Figure S14. *I*-t plots of the crystal device at 0 V bias under 50 mW.mm^{-2} light intensity (450 nm), after storage in open air for 3 months without encapsulation showing long-term environmental stability.

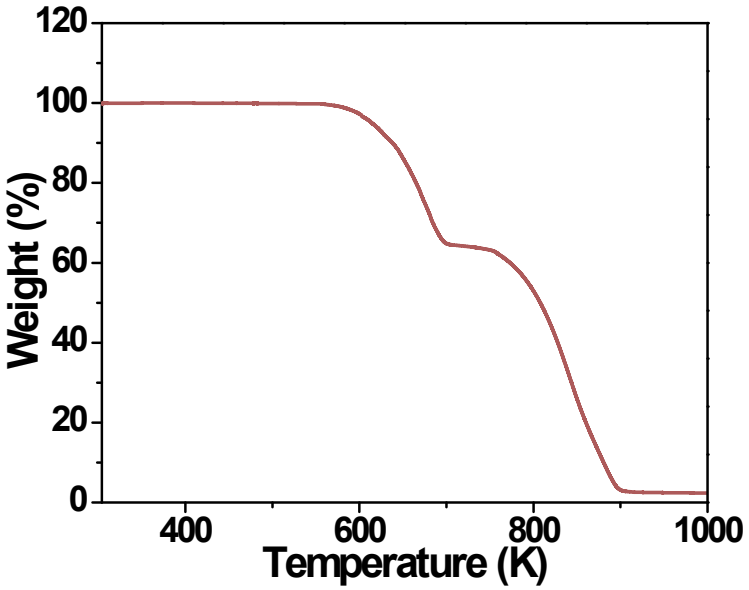

Figure S15. Thermogravimetric analysis (TGA) of (TMA)Cu_2Br_3 depicting excellent thermal stability up to ~550 K.

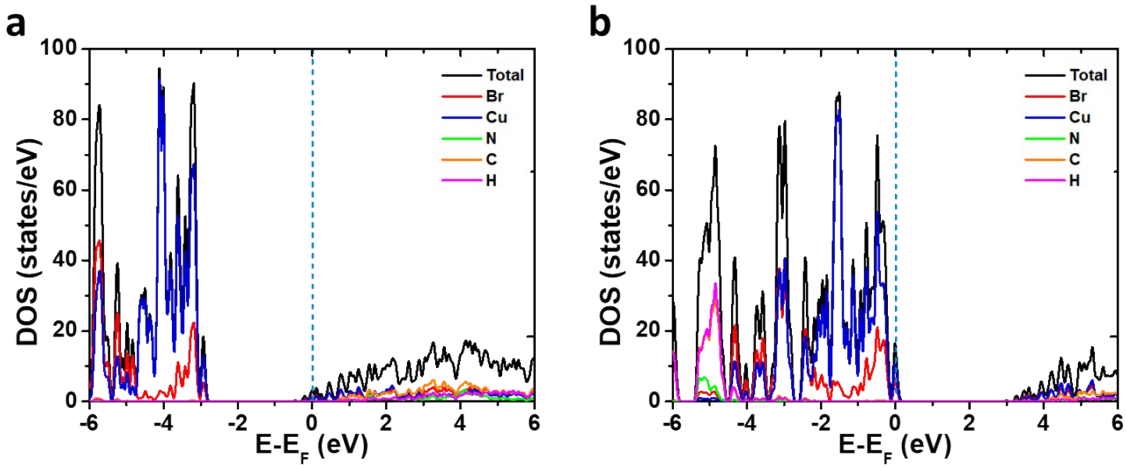

Figure S16. Atom projected density of state (DOS) plots along with the total density of state for (TMA)Cu_2Br_3 due to the (a) addition of an extra electron in the unit cell, and (b) removal of an electron (with a hole) in the unit cell.

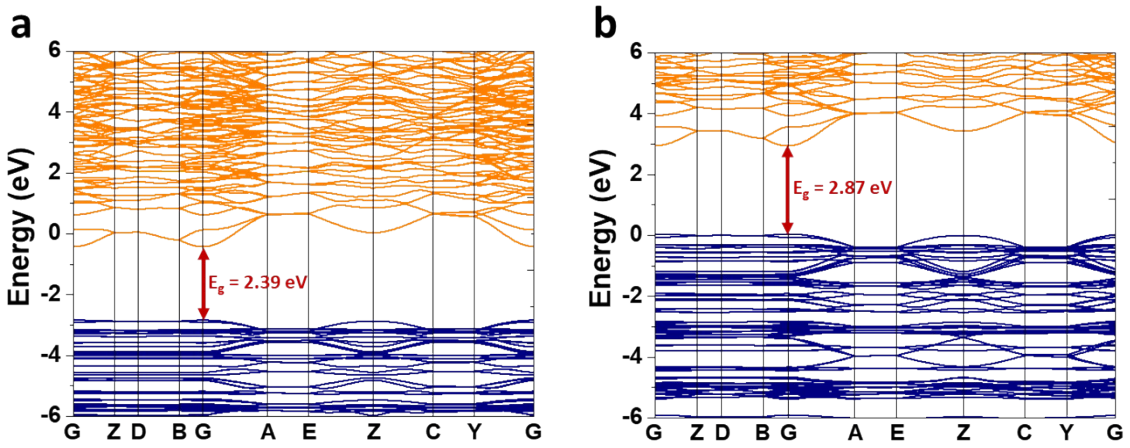

Figure S17. Electronic band structure of (TMA)Cu_2Br_3 after the (a) addition of an extra electron in the unit cell, and (b) removal of an electron (with a hole) in the unit cell.

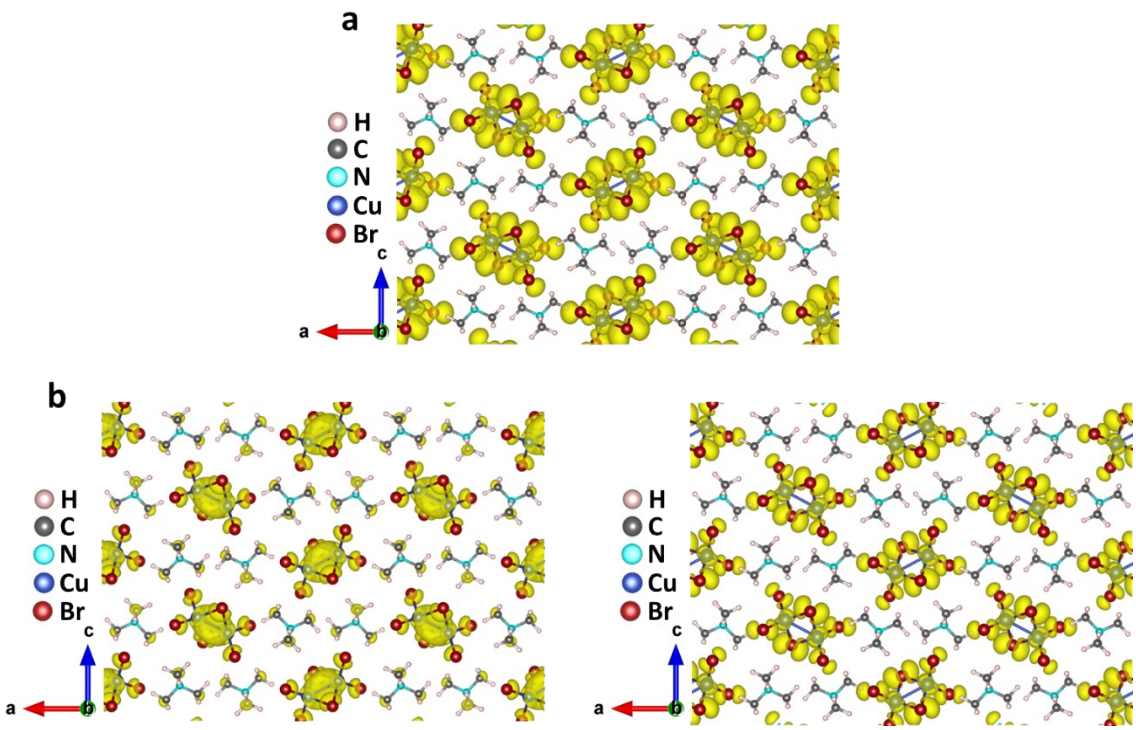

Figure S18. 2x2x2 unit cell of (TMA)Cu_2Br_3: (a) Charge density plot indicating the distribution of electronic charge before photo excitation. (b) Charge density plot indicating the distribution of electronic charge at the CBM, upon addition of an extra electron in the unit cell. (Electron accumulation is represented by yellow isosurface) (left panel). (b) Charge density plot indicating the distribution of hole charge at the VBM, upon removal of an electron (with a hole) from the unit cell (right panel).

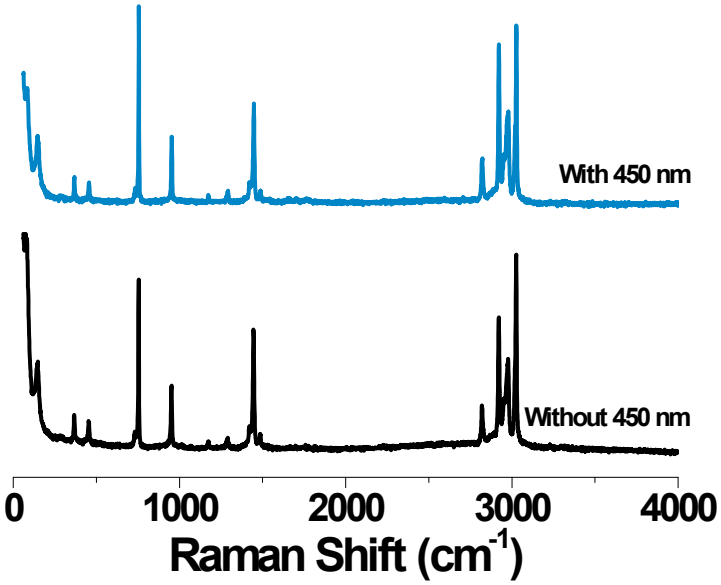

Figure S19. Comparison of full range experimental Raman spectral measurements (λ_{exc} = 632.8 nm) carried out without and with additional 450 nm laser irradiation.

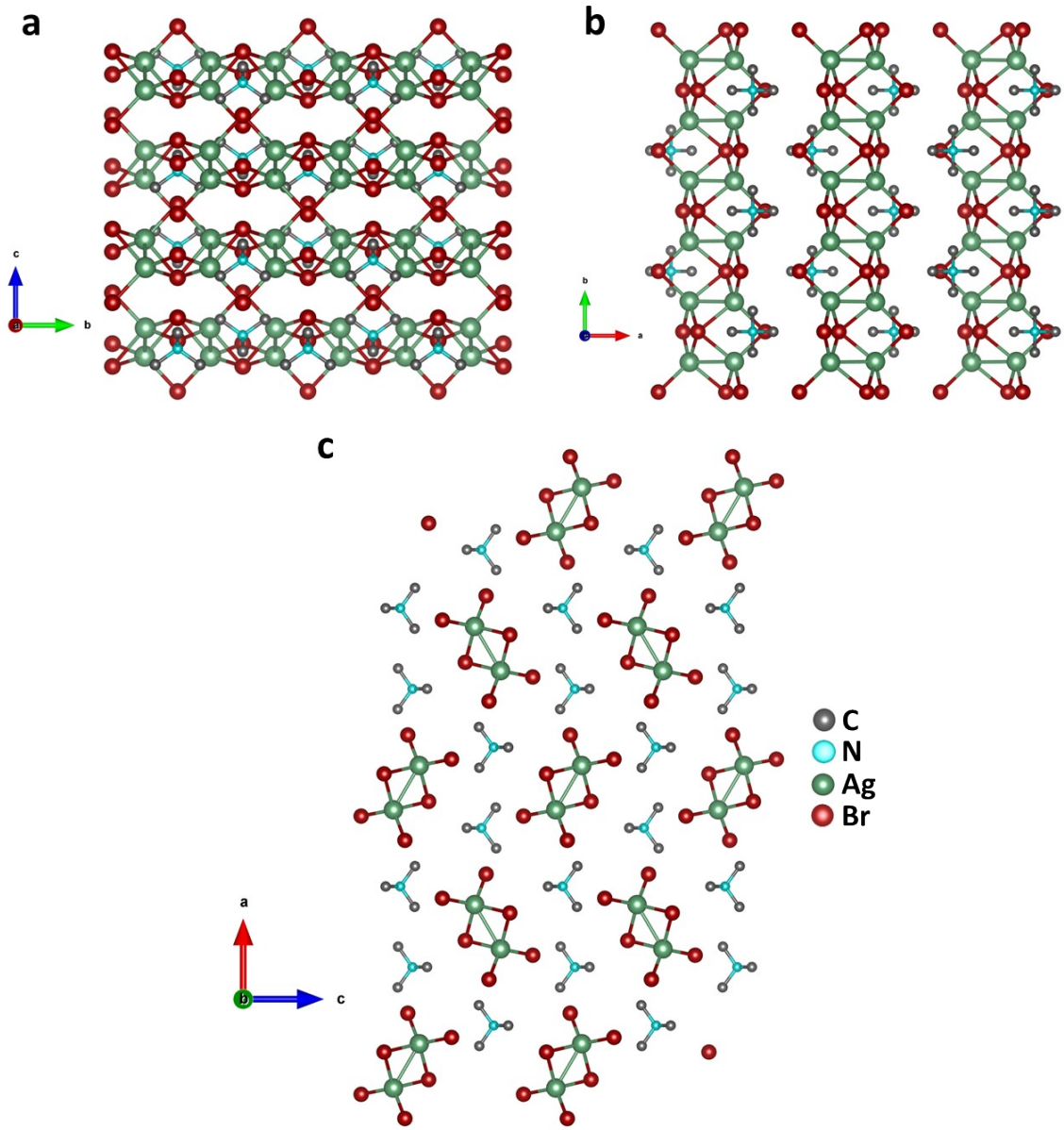

Figure S20. Crystal structure of (TMA)Ag_2Br_3 viewed along (a) a-axis, (b) c-axis, and (c) b-axis. H atoms are omitted for clarity. Each $(Ag_2Br_3)_n^{n-}$ inorganic ladder is surrounded by six stacks of TMA^+ cations.

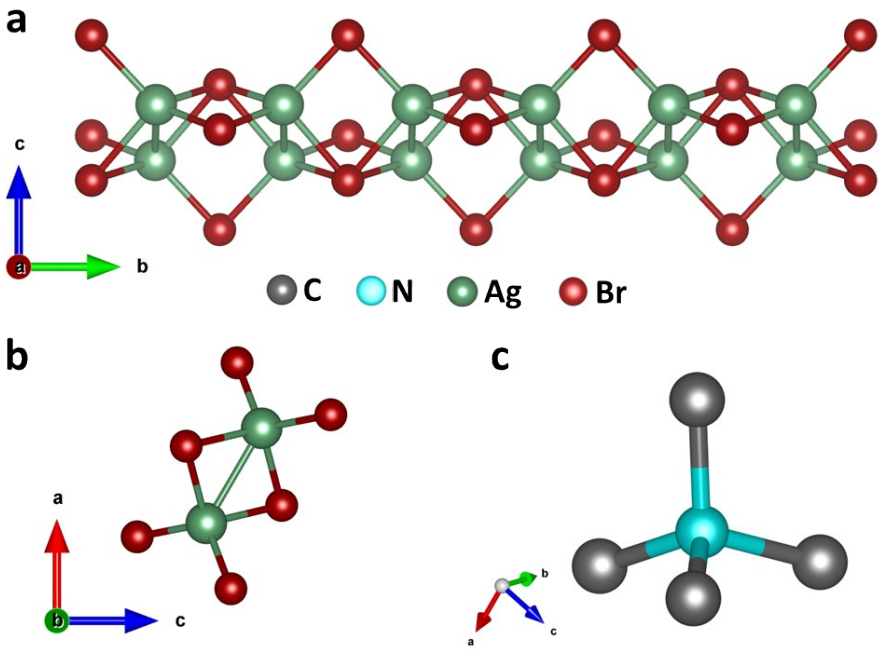

Figure S21. Polymeric chain of $(Ag_2Br_3)_n^{n-}$ anions viewed along (a) a-axis, (b) b-axis. (c) Zoomed-in view of tetramethylammonium (TMA) cation. Carbon, nitrogen, copper, and bromine atoms are represented by grey, cyan, green, and red coloured spheres.

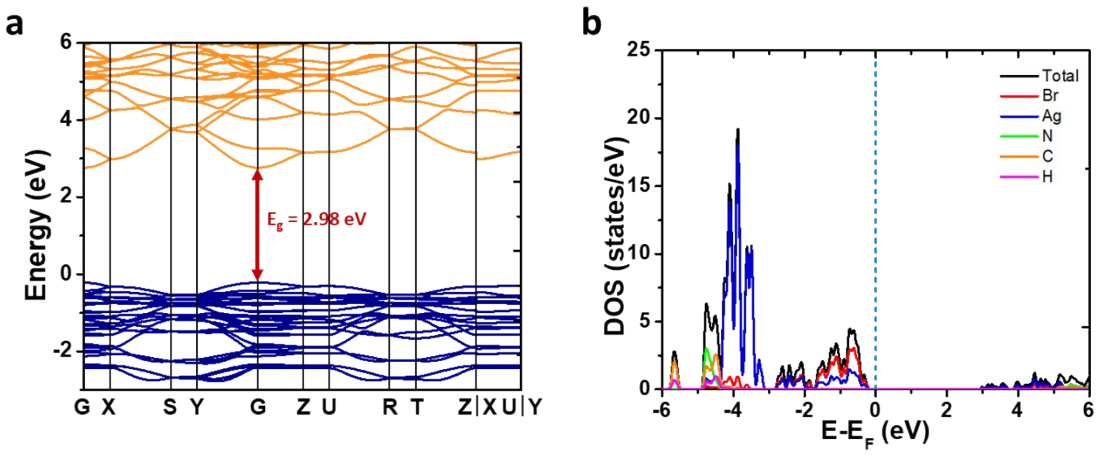

Figure S22. Electronic structure of (TMA)Ag_2Br_3. (a) Electronic band structure calculated from DFT showing direct bandgap (E_g) value of 2.98 eV at the Gamma (G) point. (b) Density of state (DOS) plots exhibiting the total as well as atomic contributions. Dotted vertical line represents the Fermi level (E_F).

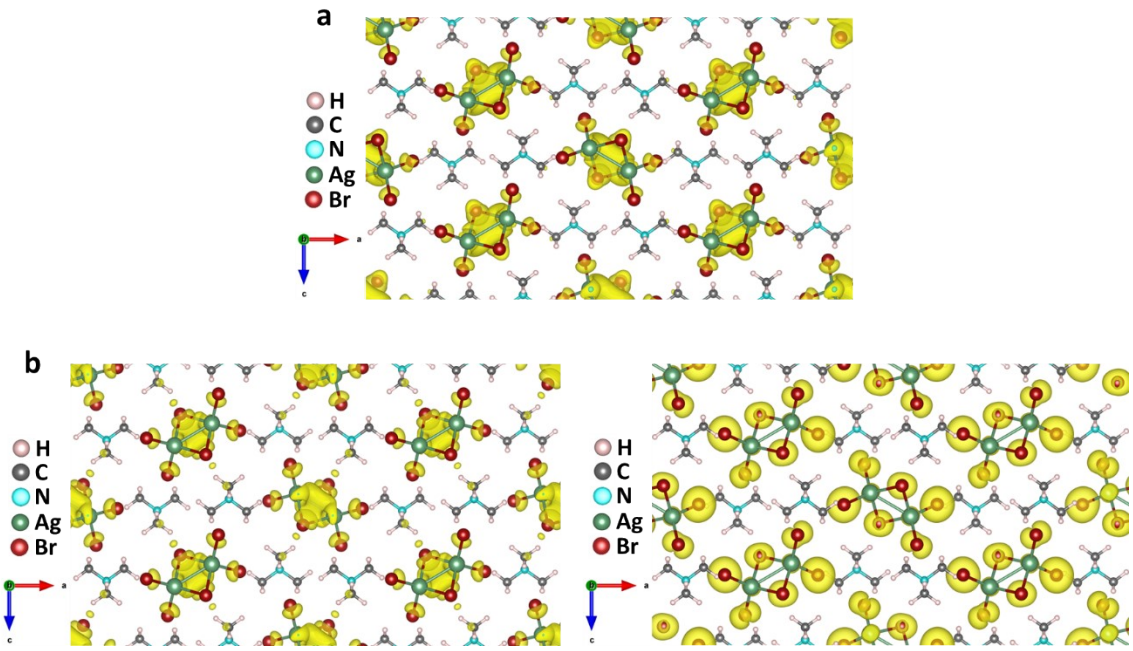

Figure S23. 2x2x2 unit cell of (TMA)Ag_2Br_3: (a) Charge density plot indicating the distribution of electronic charge before photo excitation. (b) Charge density plot indicating the distribution of electronic charge at the CBM, upon addition of an extra electron in the unit cell. (Electron accumulation is represented by yellow isosurface) (left panel). (b) Charge density plot indicating the distribution of hole charge at the VBM, upon removal of an electron (with a hole) from the unit cell (right panel).

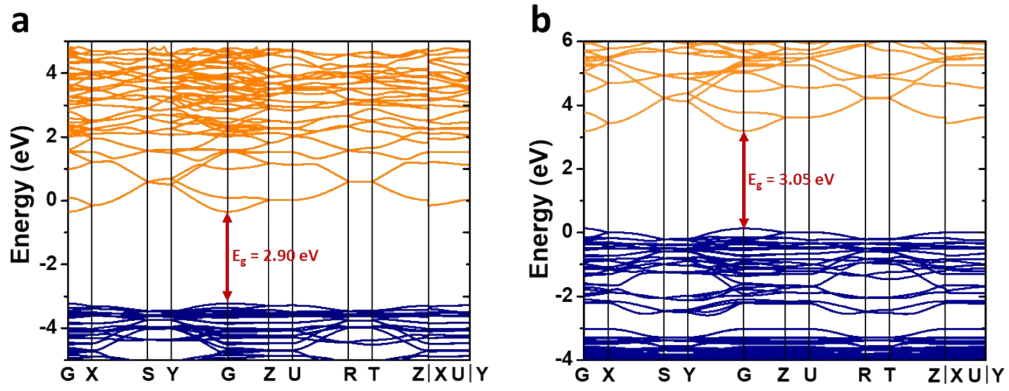

Figure S24. Electronic band structure of (TMA)Ag_2Br_3 after the (a) addition of an extra electron in the unit cell, and (b) removal of an electron (with a hole) in the unit cell.

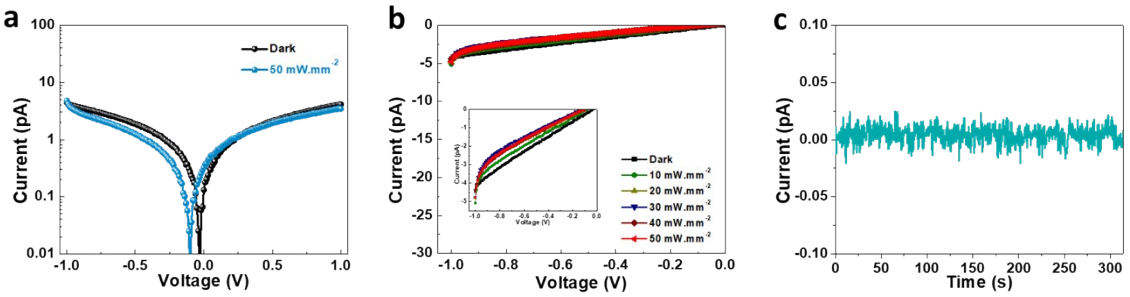

Figure S25. Photo-responsivity on the (TMA)Ag_2Br_3 system. (a) *I-V* curves in dark and under light intensity of 50 mW.mm^{-2} (450 nm). (b) *I-V* curves under varying light intensity ranging from 10 mW.mm^{-2} to 50 mW.mm^{-2} (inset: zoomed-in plots). (c) Time dependent photocurrent response under 50 mW.mm^{-2} light intensity at 0 V bias.